







## Research Article

# Protein Kinase Inhibition, Antibacterial Activity, and Characterization of Phytoextract-Mediated Silver Nanoparticles Using Aqueous Extracts of *Ifloga spicata*

Ahmad Gul,<sup>1</sup> Abdul Wahab,<sup>1</sup> Fozia Fozia ,<sup>2</sup> Syed Majid Shah,<sup>1</sup> Rukhsana Gul,<sup>3</sup> Jamshed Ali,<sup>1</sup> Nauman Rahim Khan ,<sup>1</sup> Ijaz Ahmad ,<sup>3</sup> Nisar Ahmad,<sup>4</sup> Muhammad Zia,<sup>5</sup> Riaz Ullah ,<sup>6</sup> Amal Alotaibi ,<sup>7</sup> and Mujeeb A. Sultan <sup>8</sup>

<sup>1</sup>Department of Pharmacy, Kohat University of Science & Technology, Kohat, Khyber Pakhtunkhwa, Pakistan

<sup>2</sup>Biochemistry Department, Khyber Medical University Institute of Medical Sciences, Kohat, Khyber Pakhtunkhwa, Pakistan

<sup>3</sup>Department of Chemistry, Kohat University of Science & Technology, Kohat, Khyber Pakhtunkhwa, Pakistan

<sup>4</sup>Department of Plants and Environmental Sciences, Kohat University of Science & Technology, Kohat, Khyber Pakhtunkhwa, Pakistan

<sup>5</sup>Department of Biotechnology, Quaid E Azam University, Islamabad, Pakistan

<sup>6</sup>Department of Pharmacognosy (MAPPRC), College of Pharmacy, King Saud University Riyadh, Saudi Arabia

<sup>7</sup>Department of Basic Science, College of Medicine, Princess Nourah bint Abdulrahman University, P. O. Box 84428, Riyadh 11671, Saudi Arabia

<sup>8</sup>Department of Pharmacy, Faculty of Medical Sciences, Aljanad University for Science and Technology, Taiz, Yemen

Correspondence should be addressed to Ijaz Ahmad; [drijaz\\_chem@yahoo.com](mailto:drijaz_chem@yahoo.com) and Mujeeb A. Sultan; [mujeeb.aa@just.edu.ye](mailto:mujeeb.aa@just.edu.ye)

Received 24 April 2022; Accepted 7 June 2022; Published 16 June 2022

Academic Editor: Ram Prasad

Copyright © 2022 Ahmad Gul et al. This is an open access article distributed under the Creative Commons Attribution License, which permits unrestricted use, distribution, and reproduction in any medium, provided the original work is properly cited.

This research work was focused on green synthesis of silver nanoparticles (Ag-NPs) employing an aqueous plant extract of *Ifloga spicata*. The extract of plant used in the silver nanoparticle synthesis served as a stabilizing and reducing agent. The silver nanoparticles were characterized via various techniques such as X-ray diffraction (XRD) technique, scanning electron microscopy (SEM), Fourier transform infrared (FT-IR) spectroscopy, and UV-visible spectroscopy. The FT-IR analysis showed an identification of functional groups of biomolecules present in plant extract like O-H stretching of phenolic compounds and the C-H stretch of alkanes, C=O is stretching vibration of carbonyl, C-N is stretching of amines and amides, and the C-O is stretching of ester that facilitates the formation of Ag-NPs. The spherical geometry and crystalline morphology with an average crystal size of 15-28 nm of Ag-NPs were revealed using SEM and XRD analysis, respectively. The stability of Ag-NPs was checked through changing the pH and temperature of the reaction mixture. It was examined that synthesized Ag-NPs were stable at 60°C temperatures and nearly neutral pH 8. The synthesized Ag-NPs also exhibit potential antibacterial activity that were investigated against a selected bacterial pathogens, like *E. aerogens*, *B. bronchiseptica*, and *S. typhimurium*. The silver nanoparticles exhibited a maximum zone of inhibition of 18.1 ± 1.73 mm, 14.3 ± 1.18 mm, and 19.5 ± 1.30 mm against *E. aerogens*, *B. bronchiseptica*, *S. typhimurium*, respectively. The synthesized Ag-NPs exhibit promising protein kinase inhibition at 200 (µg/mL) as compared to plant extracts.

## 1. Introduction

Metallic nanoparticles have received a significant amount of reflection over a period of time, attributed to their electronic, specific surface area, and surface atom properties. Due to

their unique physiochemical properties, metallic nanoparticles have abundantly applied in various fields, including cellular transportation, synthetic biology, and health care. Among several metal nanoparticles, Ag-NPs have received a lot of adulation as a result of their aesthetic characteristics

such as morphology, stability, and controlled geometry that can be used in various fields, such as pharmaceutical science like (diagnosis and treatment of various disease), used as a catalyst in oxidation reactions, water detoxification, agriculture, textile industries, and air filtration [1–3]. Since ancient time, silver in the form of silver sulfadiazine, silver nitrate, and metallic silver has been used for dental work, burn wound treatment, bacterial infection control, and catheters [4]. The development of Ag-NPs with a controlled structure, such as morphology, functionality, and size, is essential for a variety of biomedical applications. The physicochemical properties of any drug can be used to increase its bioavailability after systemic or localized administration of Ag-NPs [5]. The antimicrobial properties of Ag-NPs have been developed as antimicrobial drugs in wound dressing, veterinary medicine, topical ointment implants, and pharmacology. Pathogenic bacteria biofilm formation is also prevented with the use of Ag-NPs [6]. Although silver-based nanomaterials have a number of therapeutic properties, their use in biomedicine is restricted because of their toxicity and instability caused by corrosion and oxidation to the surface in an oxygen-containing biological fluid [7, 8]. The above issue may be solved via surface capping with a bioactive or biopolymer agent. Besides that, Ag-NPs improve biocompatibility and cellular uptake, as well as reducing undesirable oxidation stability and cytotoxicity that enhanced their therapeutic action [9]. Furthermore, Ag-NPs are notable for their high antibacterial activity, which is in contrast to the fact that they can kill a wide range of bacteria without causing toxicity in animal cells [10], also expressed their effectiveness in an enzyme inhibition, anticancer, and antifungal activities [11]. Ag-NPs can be synthesized using a variety of physical and chemical methods [12]. All strategies entail the use of polyols, hydrazine, trisodium citrate, ascorbic acid, and sodium borohydride, which have already reported and are well-established techniques. Even though physical and chemical methods are more effective, but these approaches may cause toxicity due to the difficulty of removing the chemicals. The chemicals and reagents used in such methods are environmentally hazardous. Therefore, the need for environmentally friendly protocols for the production of NPs sparked an interest in biogenic approaches [13, 14]. The biogenesis approach of silver nanoparticle has been introduced as an environmentally friendly, cost-effective, and high-yielding way of fabricating these nanoparticles. Thus, the environmentally safe biogenic formulation of silver nanoparticles by means of microorganisms and plant extracts is valuable for biomedical applications [15]. Therefore, various plant extracts were used for silver oxide NPs as well as ZnO-NP synthesis, as previously reported for *Berberis vulgaris* [16], *Ziziphus* [17], *Ricinus communis* leaf and root extracts [18], onion peel [19], *Grewia optiva* [20], lemon grass [21], *Rhazya stricta* [22], and *Zingiber officinale* [23] which serve as reducing and capping agents.

Multidrug-resistant (MDR) pathogens cause serious bacterial infections, which contribute throughout high morbidity and mortality. In addition, due to the inefficiency of available antibiotics, treating MDR bacterial infections in clinical biomedicine is extremely difficult [24]. In certain

cases, the antibacterial activity of available drugs is reduced due to drug instability or degradation during the digestive process. Hence, research studies have concentrated their efforts on finding novel compounds with high stability and low toxicity and to explore a system of drug delivery with higher bacterial inhibitory efficiency to target bacterial cells [25]. Improve the effectiveness of drugs and antibacterial nanoparticles by means of a drug delivery system based on polymers and exclusive properties like the size of nanoscale, which facilitate their penetration into cell membranes [26]. Similarly, protein phosphorylation through kinase controls various numbers of biological mechanisms, such as cell growth, metabolism, and signal transduction. Human genes contain over 500 protein kinase genes, accounting for about 2% of all human genes. Kinase activity modifies up to 30% of all human proteins, and kinases regulate majority of the cell functions, especially those involved in signaling pathways [27]. Despite the fact that abnormal protein phosphorylation states and kinase action have been connected to a number of diseases, including Alzheimer's disease and cancer [28]. Thus, rapid determination of protein kinase activity and promising inhibitors is important not only for providing perceptions into the fundamental biological mechanisms of diseases, but also for drug discovery and molecular-target therapies. Further, there is no specific literature available on antibacterial activity of synthesized Ag-NPs against *E. aerogens*, *B. bronchiseptica*, and *S. typhimurium*. Therefore, the above aspects emphasize the relevancy of finding new ways to tackle antibacterial and protein inhibition activities.

The present investigation is based on green synthesis source using an aqueous extract of plant *Ifloga spicata* which may act as reducing and stabilizing agent. *Ifloga spicata* belongs to the Asteraceae family of annual medicinal trees. It is observed in the desert area of Pakistan, Afghanistan, India, Canary Island, and South Spain to North Africa. The flowering season is from February to September. Some of the important phytoconstituents like alkaloids, saponins, phenolics, tannins, flavonoids, and terpenoids have been reported for *Ifloga spicata* earlier, which support the synthesis of Ag-NPs [29]. Different biological activities have been already reported by using plant extracts of various species, but in this article, we are reporting the antibacterial activity of parasites (*E. aerogens*, *B. bronchiseptica*, and *S. typhimurium*) and also to explore the protein inhibition activities of synthesized Ag-NPs that have not been reported in literature, and in this, we are reporting it for the first time. In addition, the geometry and structural investigation of synthesized silver nanoparticles was checked out by means of different techniques including scanning electron microscopy, X-ray diffractometer, Fourier transform infrared spectroscopy, and UV-Vis spectrophotometry. Furthermore, the current study also accesses potential applications in biomedical fields through green synthesized Ag-NPs for antibacterial and protein kinase inhibition activities.

## 2. Materials and Method

**2.1. Materials.** The silver nitrate was purchased as 98.9% pure chemicals from Merck, use as received with no

additional purification. Pure bacterial pathogen cultures *Enterobacter aerogenes*, *Bordetella bronchiseptica*, and *Salmonella typhimurium* were obtained from the Microbiology Department, Kohat University of Science and Technology, Kohat. Sodium hydroxide (NaOH, Daeiung), nutrient basic broth (Oxoid), sodium chloride (NaCl, Sigma-Aldrich), Cefixime (Oxoid), Surfactin (Oxoid), Mueller-Hinton agar (MHA, Oxoid), hydrochloric acid (HCl, Analar BDH), and acetone (C<sub>3</sub>H<sub>6</sub>O, Fisher Scientific) were used.

**2.2. Plant Collection and Extraction.** The plant which was collected from the District Karak, Pakistan, and was recognized by the faculty members of Department of Botany, Kohat University of Science and Technology. The collected plant was packed in polyethylene bags. After that, it was thoroughly washed and cleaned with distilled water to eliminate particulate matter and then dried in the shade room temperature. The shade-dried plants were then crushed into fine powder by mechanically using a grinder. Following that, 10 g of plant powder was dispersed in 100 mL distilled water and heated at around 30°C for 20 minutes. The aqueous extract of plants was cooled at room temperature before being filtered over a Whatman No. 1 filter paper. The filtrate was used to reduce Ag<sup>+</sup> to Ag<sup>0</sup> ion.

**2.3. Preparation of AgNO<sub>3</sub> Solution.** For the preparation of a (0.1 Mm) solution of silver nitrate (AgNO<sub>3</sub>), dissolve 0.7644 g of AgNO<sub>3</sub> in 450 mL of distilled water. Impurities were kept out of the beaker by using an aluminium file. To ensure that the AgNO<sub>3</sub> crystals were properly saturated, the reaction was stirred constantly. A freshly prepared silver nitrate solution was used for the Ag-NP synthesis.

**2.4. Green Synthesis of Ag-NPs.** Various concentration ratios of plant extract and precursor, including 1:1, 3:1, 5:1, 7:1, 9:1, 1:3, 1:5, 1:7, and 1:9, were used for Ag-NP synthesis. The solution was stirred for 10 minutes at 200 rpm and a temperature of 20-25°C in a rotatory orbital shaker. The colour changes from green to dark brown after a few minutes, indicating that the reduction silver ion that was responsible for Ag-NP synthesis. In order to confirm the absorption spectra of green synthesized Ag-NPs, the UV-visible spectrophotometer was used to get the optimized ratio. Samples were centrifuged at an optimized ratio for 30 minutes and stirred at 4000 rpm. After centrifugation, a solid Ag-NP was obtained. The pellet containing Ag-NPs was then washed three times using distilled water, acetone, ethanol, and methanol to eradicate any remaining impurities. The powder form of Ag-NPs was further utilized for characterization and their biomedical applications [30].

**2.5. Characterization.** A spectrophotometer (Shimadzu UV-1800, Japan) that measures UV-visible light was employed to monitor the reduction of AgNO<sub>3</sub> ions in solution by taking an infrared spectrum of the samples at wavelengths ranging from 190 to 800 nm. An X-ray diffractometer (Rigaku MiniflexII) was used to investigate the lattice parameter of metallic silver nanoparticles. The samples were tested in the 2θ range of 10-80° and using CuK radiation (=1.5406), at a current of 40 mA and a voltage of 40 kV with a 5°/min scan-

ning speed and a size of 0.02°. To investigate the geometrical examination of nanoparticles, SEM analysis was used. The sample was prepared by simply dropping a very small amount of the thin films sample on a carbon-coated copper grid and trying to wipe away any excess solution with blotting paper, and then, the mercury lamp was used to dry the film on the grid of scanning electron microscope for 5 minutes. FT-IR analysis is used to examine the functional group identification of Ag-NPs, because every chemical bond has band absorption energy, which is used to study the bond details of compounds in order to determine the bonding type and strength. The KBr pellet method was used to obtain FT-IR spectra of synthesized samples with a resolution of 4 cm<sup>-1</sup> in the range of 4000-400 cm<sup>-1</sup> [31].

## 2.6. Biological Assays

**2.6.1. Antibacterial Activity.** The biosynthesis Ag-NPs were screened against the subsequent bacterial strains *E. aerogenes*, *B. bronchiseptica*, and *S. typhimurium* using the disc diffusion protocol [32]. The reason for choosing these strains is that they are common pathogens that are resistant to many antibiotics and can inhibit various diseases, including intestinal and skin infections. The selected bacterial strains were placed in test tubes impregnated with water and peptone. Inoculation was done using a sterile wire loop. The inoculum concentration was the same as McFarland's 0.5 standard. The media Mueller-Hinton agar was used that allows for better antibiotic diffusion than most of the other plates and also exhibits an effective zone of inhibition. The culture media were prepared by dissolving 28 g of Mueller-Hinton agar (MHA) in 1 L of double-distilled water, heated for 20 minutes in order to completely solubilize the media contents, and then autoclaved for 15 minutes at 15 psi pressure and 121°C temperature to completely sterilize the medium. After sterilization, the medium was solidified by cooling at about 45°C. An aqueous solution with the fixed concentration of NP was prepared. Sterile paper discs (5 mm), immersed in colloidal solution and pure water (negative control), were placed on the agar plate. After incubation for 24 hours at 37°C, the inhibition zone for each sample was recorded using Cefixime as positive control.

**2.6.2. Protein Kinase Inhibition Activity.** The following protocol was used to assess receptivity to Streptomyces 85E strains that use kinase for hyphae development and formation. The strain was inoculated into tryptic soy broth and allowed to refresh for 24-48 hours. The revived culture was then swabbed over mineral ISP4 media, and sample infused filter paper discs (5 L of 20 mg/mL DMSO) were positioned in the seeded plates and properly labelled. As positive and negative controls, surfactant containing sporulation inhibitor and DMSO impregnated discs were used. The plates were then incubated for 48-72 hours at 28°C to allow for hyphae development, and a vernier caliper was used to measure the clear or the bald zone of growth inhibition around the discs. The existence of clear or bald areas around the disc demonstrates that phosphorylation has been inhibited, which in turn has precluded the formation of mycelium

and spores. The ability of the sample to inhibit mycelial formation is indicated by bald areas, whereas the blank area indicates cytotoxicity and the lethality of test samples [11, 33].

### 3. Results and Discussion

According to reported literature, the dark brown solution of silver nanoparticles and the establishment of pigment is because of the excitation of surface plasmonic resonance process of Ag-NPs. By mixing the aqueous extracts of *Ifloga spicata* with the AgNO<sub>3</sub> solution, the colour changed was observed from green to and dark brown within a few minutes. This colour shift is due to the alignment of Ag-NPs. A UV-visible spectrophotometer was used to investigate the reduction of pure Ag ions into metal-NPs, which confirmed the synthesis of silver nanoparticles during the reaction. For the identification of samples, the irradiation range was 400–800 nm, whereas the used solvent in a UV-visible spectrophotometer was double-distilled water and to attain ostensible peak, the quartz cuvettes were used [34].

**3.1. UV-Visible Spectroscopy.** The first confirmatory test for the silver nanoparticle synthesis was examined under an ultraviolet spectrophotometric analysis. The absorption peaks in the wavelength of 400–475 nm were measured to investigate the synthesis of silver nanoparticles. Different volumes of sample AgNO<sub>3</sub> and plant extracts were examined in order to obtain the best ultraviolet spectra. The solution of plant extracts and silver nanoparticles was mixed in various ratios including 1:1, 3:1, 5:1, 7:1, 9:1, 1:3, 1:5, 1:7, and 1:9 (Figure 1). The UV-visible spectra of samples with a 1:9 ratio of plant extracts to AgNO<sub>3</sub> yielded the most dominant, sharp, and intense peak at 440 nm, as shown in Figure 2. This sample concentration ratio was chosen to ensure that the maximum amount of silver ions was converted to metallic silver nanoparticles. UV-visible studies of nanoparticles confirmed the synthesis and the long-term stability particles. Further, Faisal et al., Singh et al., and Banerjee et al. have all reported similar findings [2, 4, 35].

**3.1.1. UV-Visible Analysis at Disparate pH and Temperature.** Stability is a primary consideration for the formation of nanoparticles. Due to their distribution, shape, and size change as the external conditions of the reaction changes. Therefore, assessing the stability of biosynthetic nanoparticles is very important at different temperature and pH levels. An ultraviolet-visible spectrophotometer was used to examine optimal ratios in different range of temperature (20–100°C) and pH (2–12). According to the pH spectrum, silver nanoparticles were more stable in alkaline media, whereas acids act as an oxidizing agent in an acidic environment, resulting the formation of highly unstable NPs. One of most pronounced peaks was identified at (pH 8), which is fairly close to the neutral pH range. Hence, such pH range is suitable for stable synthesis of silver nanoparticles and also applied in various applications. Stability of the silver nanoparticles showed varied by altering the pH of the solution, as shown in Figure 3. The reaction mixture can also affect the synthesis of nanoparticles by changing the temperature.

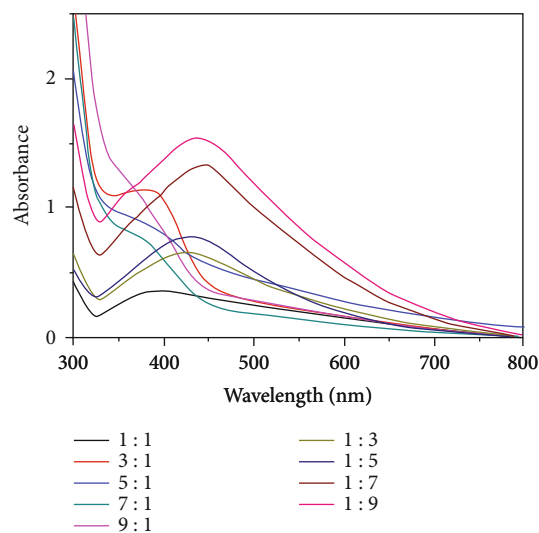


FIGURE 1: UV-Vis graph at different ratio of the plant extracts and AgNO<sub>3</sub>.

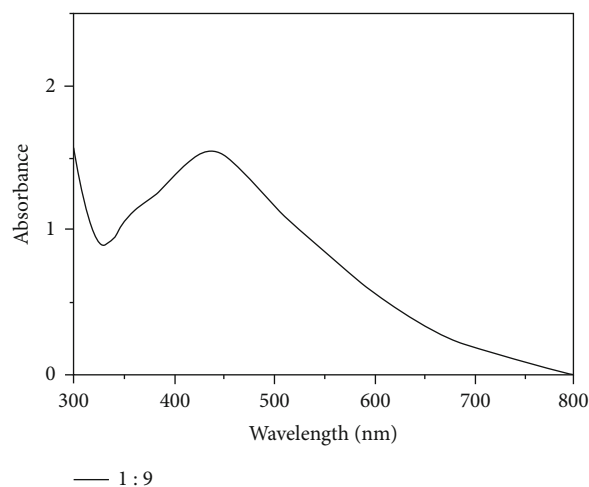


FIGURE 2: Peak for maximum ratio of 1:9 for plant extracts and AgNO<sub>3</sub>.

As a result, NPs were synthesized at various temperatures and examined under visible analysis. Figure 4 depicts the recorded spectrum of Ag-NPs at different temperature. Ag-NPs were found to be stable at moderate temperatures (40–80°C) that were analyzed by a visible analytical spectrum in Figure 4. The maximum absorption peak was found at the 60°C with a small increase in temperature can cause a very stable synthesis Ag-NPs. Therefore, the optimized temperature for stable Ag-NP synthesis was observed at 60°C, because it requires less amount of heat. According to Borase et al., a small increase in temperature has a positive effect on Ag-NP synthesis and stability [30, 36].

**3.2. FT-IR Spectroscopy.** A Perkin-Elmer FT-IR spectrophotometer with a scanning range of 400–4000 cm<sup>-1</sup> was used to specify different biomolecules or functional groups involved in the nanoparticle synthesis. In this analysis, plant



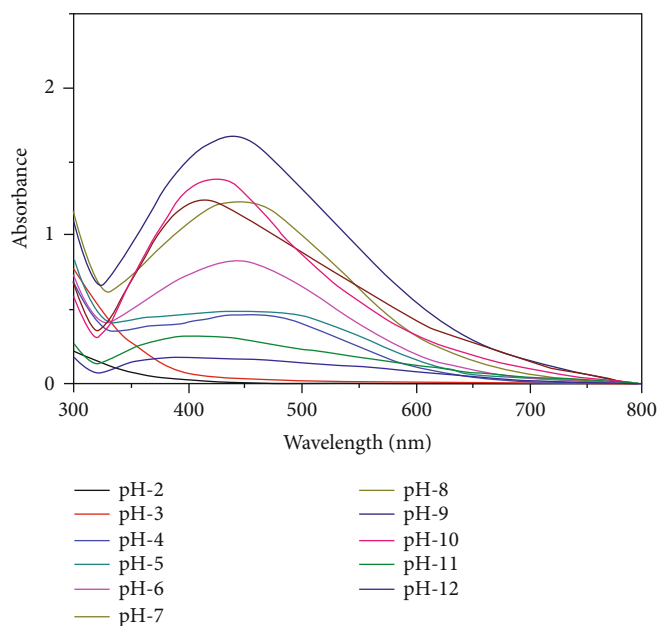


FIGURE 3: UV result at different pH from 2 to 12 of biosynthesized silver nanoparticles.

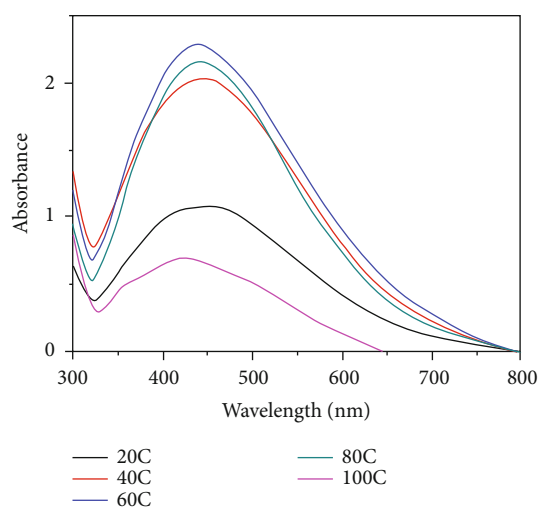


FIGURE 4: UV-Vis results for Ag-NPs with different temperature from 20 to 100°C.

extracts were utilized to determine the different functional groups that help in the stabilization and reduction of Ag-NPs. Figure 5 demonstrates the spectroscopic plot. The purpose of FT-IR spectroscopic analysis was to detect the existence of metabolites that are capable for the Ag ion reduction. The broad absorption band at  $3266\text{ cm}^{-1}$  was referred to as the stretching vibration of O-H of phenolic and alcoholic compounds. The stretching vibration of C-H in alkanes is depicted by the band at  $2927\text{ cm}^{-1}$ . The stretching vibration of C=O in ketone, carboxylic acid, and aldehydes is reflected by the  $1715\text{ cm}^{-1}$  band. The C=C stretching vibration of diketone (aromatic ring) attributed the band at  $1589\text{ cm}^{-1}$ . The absorbance band located at  $1377\text{ cm}^{-1}$  was the C-H bending vibration of alkanes. The

peak around  $1259$  and  $1167\text{ cm}^{-1}$  may be allotted is the C-N and C-O stretching of amines, amides (alkyl amine), ester, and carbonyl. The band at  $1046\text{ cm}^{-1}$  indicates the C-O stretching of ester and carbonyl. The band shift was observed at  $3249\text{ cm}^{-1}$ ,  $2917\text{ cm}^{-1}$ ,  $1541\text{ cm}^{-1}$ ,  $1376\text{ cm}^{-1}$ ,  $1235\text{ cm}^{-1}$ , and  $1005\text{ cm}^{-1}$  indicating the phytochemicals that are involved in the silver ion reduction and stabilization process. The FT-IR results of both Ag-NPs and the plant extracts confirmed the biomolecule responsible for the reduction  $\text{Ag}^+$  ions into  $\text{Ag}^0$  are primarily flavonoids, proteins, and polyphenolic compounds [2, 37, 38].

**3.3. XRD Pattern.** The crystal structure, size, and shape of Ag-NPs were ascertained employing an XRD pattern. The XRD pattern of silver nanoparticles was performed in the range  $2\theta$  degree of  $20^\circ$  to  $80^\circ$ . Figure 6 depicts the result of the obtained Ag-NPs. XRD analysis discovered four strong peaks of diffraction at  $38.05^\circ$ ,  $44.25^\circ$ ,  $64.6^\circ$ , and  $77.3^\circ$ , which correspond to the Bragg diffraction peak values of (111), (200), (220), and (311), respectively. The attained pattern demonstrates that silver nanoparticles have a face-centered cubic structure. The most significant peak on the diffractogram was observed at  $38.05^\circ$  at  $2\theta$ , indicating that the top-most crystal plane, which is the basal plane of (111) for Ag-NPs. The particle size of synthesized Ag-NPs ranges from 15 to 28 nm, calculated by using Scherrer's equation.

$$D = \frac{k\lambda}{\beta \cos\theta}, \quad (1)$$

where crystalline size (nm) is represented by  $D$ , Scherrer's constant is denoted by  $K$  (value ranging from 0.9 to 1),  $\lambda$  refers the wavelength,  $\beta$  is the full width and half maximum (FWHM), and  $\theta$  is Bragg's angle of diffraction in degree [39].

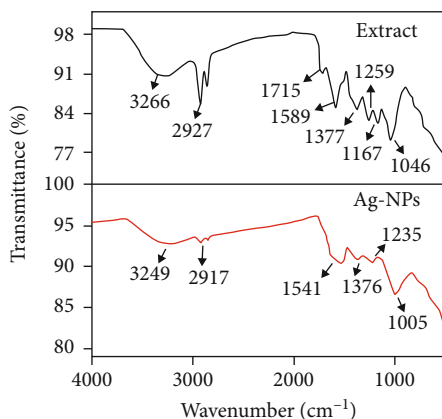


FIGURE 5: Combined FTIR spectra of silver-NPs and plant extracts.

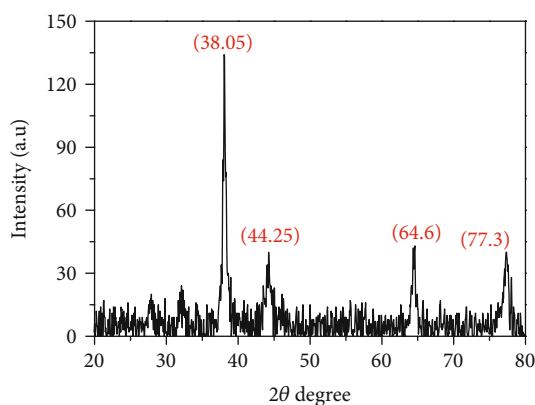


FIGURE 6: XRD pattern of synthesized Ag-NPs.

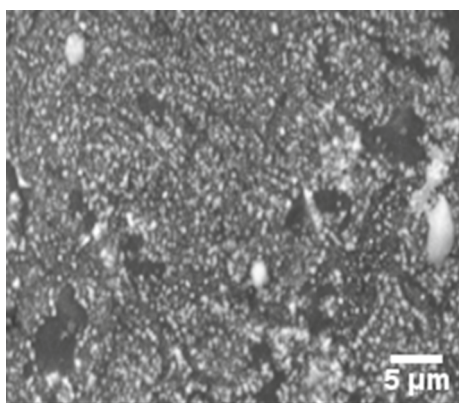


FIGURE 7: SEM result for synthesized silver-NPs.

**3.4. SEM Analysis.** SEM examination was performed using a microscope Jeol, Japan, Model-6360 to evaluate the morphology, topography, and size of newly green synthesized silver nanoparticles [4, 40]. SEM micrographs of silver nanoparticles are shown in Figure 7; the images exhibit that almost all of the particles were well dispersed in the medium and exhibit spherical morphology. According to the examination of silver nanoparticles, the average particle size in

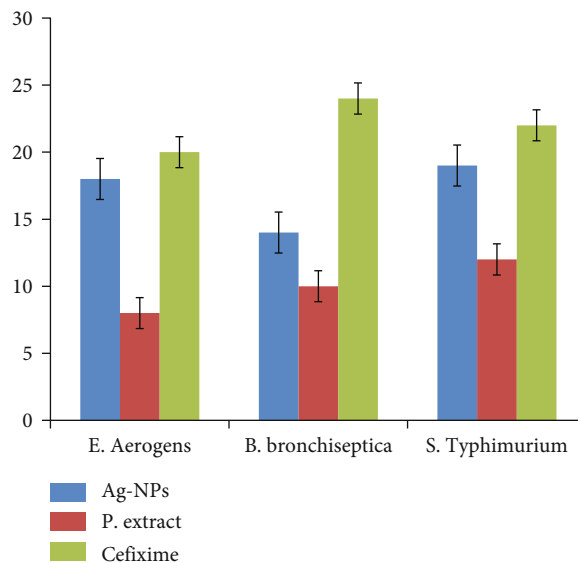


FIGURE 8: Comparison of Ag-NPs, extracts, and standard antibacterial activities.

the medium was 10–60 nm, which is consistent with XRD particle sizes of 15–28 nm.

### 3.5. Biological Activity Analysis

**3.5.1. Antibacterial Activity Ag-NPs.** Silver nanoparticles had a successful antimicrobial agent that can be used to stop infection of orthopedic implants. The standard Agar Well diffusion technique was used to check the effectiveness of integrated Ag-NPs toward antibacterial activity. The probable bacterial activity against different bacterial strain was determined via plant extract and Ag-NPs. Three bacterial strains, *E. aerogens*, *B. bronchiseptica*, and *S. typhimurium*, were used which are liable for a variety of diseases, mainly include intestinal infections and skin infections. It was observed that Ag-NPs were more effective against *E. aerogens*, *B. bronchiseptica*, and *S. Typhimurium* bacterial strains, as shown in Figure 8. The sample exhibits a maximum zone of inhibition of  $18.1 \pm 1.73$  mm,  $14.3 \pm 1.18$  mm, and  $19.5 \pm 1.30$  mm against *E. aerogens*, *B. bronchiseptica*, and *S. typhimurium*, respectively, while the plant extract exhibits minimum inhibition  $8.2 \pm 1.41$  mm,  $10.2 \pm 1.46$  mm, and  $12.3 \pm 1.21$  mm as compared to newly synthesized Ag-NPs. The standard drug, Cefixime, came up with the bacterial inhibition of  $20.1 \pm 1.11$  mm,  $24.2 \pm 1.44$  mm, and  $22.1 \pm 1.12$  mm against *E. aerogens*, *B. bronchiseptica*, and *S. typhimurium*, respectively. When the plant extracts were compared to silver nanoparticles and a standard drug, the Ag-NPs from the same plant showed excellent antibacterial activity against *E. aerogens*, *B. bronchiseptica*, and *S. typhimurium* bacterial strains [41–43]. It is essential to verify the effect of sample in biomedical applications. Our findings suggest that *B. bronchiseptica* is less efficient than other parasites because Ag-NPs do not damage DNA, so rupture of the cell membrane by Ag-NPs could be one of the causes of cell death of parasite. The result indicates that synthesized Ag-NPs showed no damage

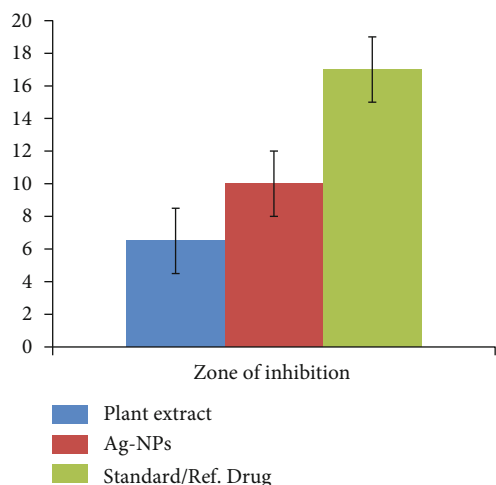


FIGURE 9: Comparison of Ag-NPs, extract, and standard protein kinase inhibition activities.

of DNA within this concentration range. Therefore, synthesized Ag-NPs exhibit good antibacterial activity against *E. aerogens* and *S. typhimurium* bacterial strains compared to *B. bronchiseptica* [44].

**3.5.2. Protein Kinase Inhibition Activity.** One of the most essential techniques used to control a variety biological processes is the phosphorylation of tyrosine and threonine/serine protein kinase. These processes include cell differentiation, cell proliferation, apoptosis, and metabolism. The uncontrolled phosphorylation of these metabolic reactions generally begins during tumorigenesis, which is frequently caused by genetic changes that lead to cancer. According to this analysis, protein kinase has been identified as a potential target for inhibiting critical cancer disease. *Streptomyces* sp. aerial hyphae formation is essential for the action of protein kinase. Ag-NPs also act as a protein kinase inhibitors which may inhibit the growth of *Streptomyces* sp. aerial hyphae [45]. Thus, the phosphorylation inhibition and final production of spores and mycelium were determined using visual indicators such as the appearance of clear or bald areas over a disc. The potent inhibition of mycelium formation of the test sample was specified bald area, which showed  $6.5 \pm 1.91$  mm for plant extracts,  $17.3 \pm 0.83$  mm for drug (Surfactin), and  $10.1 \pm 1.27$  mm for Ag-NPs at concentration of  $200 \mu\text{g/mL}$ , respectively (Figure 9), whereas the clear area indicated the strain death and the cytotoxicity of the sample. Hence, we conclude that when plant extracts and Ag-NPs were tested against *Streptomyces* strains, Ag-NPs were more effective inhibitors than plant extracts.

## 4. Conclusion

According to the current study, the silver nanoparticle synthesis was successfully achieved using an aqueous extract of *Ifloga spicata* that contains a number of compounds serves as a capping and reducing agents. The average particle size of silver nanoparticles was found between 15 and 28 nm. Even though the pH and temperature of the reaction were

changed to improve the size and shape of the nanoparticles. The Ag-NPs were stable at high temperatures ( $60^\circ\text{C}$ ) and neutral, basic pH 8, while unstable at acidic pH. The SEM images revealed that Ag-NPs are spherical in shape. The FT-IR results indicate that different bioactive compounds were involved in reduction of  $\text{Ag}^+$ . Furthermore, the synthesized Ag-NPs also have probable antimicrobial and protein kinase inhibitory properties. In comparison to plant extract, Ag-NPs showed excellent results against the *Salmonella typhimurium* bacterial strain, while in protein kinase inhibition, silver nanoparticles showed the maximum zone of inhibition. Many aspects of this goal are still unsolved, and future research may aid in overcoming current hurdles. We suggest that the researcher should explore the proposed mechanisms of the action, and synthesized Ag-NPs may be able to solve the problem of toxicity and also prevent the development of resistance.

## Data Availability

All the available data are incorporated in the MS.

## Conflicts of Interest

The authors declare that there are no competing financial interests.

## Acknowledgments

The authors wish to thank Princess Nourah bint Abdulrahman University Researchers Supporting Project number (PNURSP2022R33), Princess Nourah bint Abdulrahman University, Riyadh, Saudi Arabia, for financial support.

## References

- [1] M. R. Shaik, M. Khan, M. Kuniyil et al., "Plant-extract-assisted green synthesis of silver nanoparticles using *Origanum vulgare* L. extract and their microbicidal activities," *Sustainability*, vol. 10, no. 4, p. 913, 2018.
- [2] S. Faisal, M. Rizwan, R. Ullah et al., "Paraclostridium benzoe-lyticum bacterium-mediated zinc oxide nanoparticles and their in vivo multiple biological applications," *Oxidative Medicine and Cellular Longevity*, vol. 2022, 15 pages, 2022.
- [3] N. Ahmad, M. Jabeen, Z. U. Haq et al., "Green fabrication of silver nanoparticles using *Euphorbia serpens* Kunth aqueous extract, their characterization, and investigation of its in vitro antioxidative, antimicrobial, insecticidal, and cytotoxic activities," *BioMed Research International*, vol. 2022, 11 pages, 2022.
- [4] A. Singh, D. Jain, M. Upadhyay, N. Khandelwal, and H. Verma, "Green synthesis of silver nanoparticles using *Argemone mexicana* leaf extract and evaluation of their antimicrobial activities," *Digestive Journal of Nanomaterials and Bioscience*, vol. 5, pp. 483–489, 2010.
- [5] C. Baker, A. Pradhan, L. Pakstis, D. J. Pochan, and S. I. Shah, "Synthesis and antibacterial properties of silver nanoparticles," *Journal of Nanoscience and Nanotechnology*, vol. 5, no. 2, pp. 244–249, 2005.
- [6] S. Pounraj, P. Somu, and S. Paul, "Chitosan and graphene oxide hybrid nanocomposite film doped with silver nanoparticles

- efficiently prevents biofouling,” *Applied Surface Science*, vol. 452, pp. 487–497, 2018.
- [7] L. Wang, T. Zhang, P. Li et al., “Use of synchrotron radiation-analytical techniques to reveal chemical origin of silver-nanoparticle cytotoxicity,” *ACS Nano*, vol. 9, no. 6, pp. 6532–6547, 2015.
- [8] C. Marambio-Jones and E. Hoek, “A review of the antibacterial effects of silver nanomaterials and potential implications for human health and the environment,” *Journal of Nanoparticle Research*, vol. 12, no. 5, pp. 1531–1551, 2010.
- [9] E. Panzarini, S. Mariano, C. Vergallo et al., “Glucose capped silver nanoparticles induce cell cycle arrest in HeLa cells,” *Toxicology In Vitro*, vol. 41, pp. 64–74, 2017.
- [10] O. E. Elshawy, E. A. Helmy, and L. A. Rashed, “Preparation, characterization and in vitro evaluation of the antitumor activity of the biologically synthesized silver nanoparticles,” *Advances in Nanoparticles*, vol. 5, no. 2, pp. 149–166, 2016.
- [11] S. Khan, T. Ur-Rehman, B. Mirza, I. Ul-Haq, and M. Zia, “Antioxidant, antimicrobial, cytotoxic and protein kinase inhibition activities of fifteen traditional medicinal plants from Pakistan,” *Pharmaceutical Chemistry Journal*, vol. 51, no. 5, pp. 391–398, 2017.
- [12] A. Prusty and P. Parida, “Development and evaluation of gel incorporated with biogenically Synthesised silver nanoparticles,” *Journal of Applied Biology Pharmacology*, vol. 3, no. 1, pp. 1–6, 2015.
- [13] A. Nabikhan, K. Kandasamy, A. Raj, and N. M. Alikunhi, “Synthesis of antimicrobial silver nanoparticles by callus and leaf extracts from saltmarsh plant, *Sesuvium portulacastrum* L.,” *Colloids and Surfaces B: Biointerfaces*, vol. 79, no. 2, pp. 488–493, 2010.
- [14] K. Logaranjan, A. J. Raiza, S. C. Gopinath, Y. Chen, and K. Pandian, “Shape-and size-controlled synthesis of silver nanoparticles using Aloe vera plant extract and their antimicrobial activity,” *Nanoscale Research Letters*, vol. 11, no. 1, pp. 1–9, 2016.
- [15] M. Aslam, F. Fozia, A. Gul et al., “Phyto-extract-mediated synthesis of silver nanoparticles using aqueous extract of *Sanvitalia procumbens*, and characterization, optimization and photocatalytic degradation of azo dyes Orange G and Direct Blue-15,” *Molecules*, vol. 26, no. 20, p. 6144, 2021.
- [16] M. Behravan, A. H. Panahi, A. Naghizadeh, M. Ziaee, R. Mahdavi, and A. Mirzapour, “Facile green synthesis of silver nanoparticles using *Berberis vulgaris* leaf and root aqueous extract and its antibacterial activity,” *International Journal of Biological Macromolecules*, vol. 124, pp. 148–154, 2019.
- [17] M. L. Guimarães, F. A. G. da Silva, M. M. da Costa, and H. P. de Oliveira, “Green synthesis of silver nanoparticles using *Ziziphus joazeiro* leaf extract for production of antibacterial agents,” *Applied Nanoscience*, vol. 10, no. 4, pp. 1073–1081, 2020.
- [18] A. Gul, A. Shaheen, I. Ahmad et al., “Green synthesis, characterization, enzyme inhibition, antimicrobial potential, and cytotoxic activity of plant mediated silver nanoparticle using *Ricinus communis* leaf and root extracts,” *Biomolecules*, vol. 11, no. 2, p. 206, 2021.
- [19] Y. H. Yap, A. A. Azmi, N. K. Mohd et al., “Green synthesis of silver nanoparticle using water extract of onion peel and application in the acetylation reaction,” *Arabian Journal for Science and Engineering*, vol. 45, no. 6, pp. 4797–4807, 2020.
- [20] M. Iftikhar, M. Zahoor, S. Naz et al., “Green Synthesis of Silver Nanoparticles Using *Grewia optiva* Leaf Aqueous Extract and Isolated Compounds as Reducing Agent and Their Biological Activities,” *Journal of Nanomaterials*, vol. 2020, 10 pages, 2020.
- [21] H. Agarwal, S. V. Kumar, and S. Rajeshkumar, “Antidiabetic effect of silver nanoparticles synthesized using lemongrass (*Cymbopogon Citratus*) through conventional heating and microwave irradiation approach,” *Journal of Microbiology, Biotechnology and Food Sciences*, vol. 7, no. 3, pp. 371–376, 2018.
- [22] S. Najoom, F. Fozia, I. Ahmad et al., “Effective antiplasmodial and cytotoxic activities of synthesized zinc oxide nanoparticles using *Rhazya stricta* leaf extract,” *Evidence-based Complementary and Alternative Medicine*, vol. 2021, 9 pages, 2021.
- [23] N. S. Al-Radadi, S. Faisal, A. Alotaibi et al., “Zingiber officinale driven bioproduction of ZnO nanoparticles and their anti-inflammatory, anti-diabetic, anti-Alzheimer, anti-oxidant, and anti-microbial applications,” *Inorganic Chemistry Communications*, vol. 140, p. 109274, 2022.
- [24] M. Vazirian, K. Hamidian, M. Noorollah, and A. Manayi, “Enhancement of antibiotic activity and reversal of resistance in clinically isolated methicillin-resistant *Staphylococcus aureus* by *Trachyspermum ammi* essential oil,” *Research Journal of Pharmacognosy*, vol. 6, no. 1, pp. 1–10, 2019.
- [25] J. Marto, H. M. Ribeiro, and A. J. Almeida, “Starch-based nanocapsules as drug carriers for topical drug delivery,” *Smart Nanocontainers*, pp. 287–294, 2020.
- [26] S. Vrignaud, J. P. Benoit, and P. Saulnier, “Strategies for the nanoencapsulation of hydrophilic molecules in polymer-based nanoparticles,” *Biomaterials*, vol. 32, no. 33, pp. 8593–8604, 2011.
- [27] S. Xu, Y. Liu, T. Wang, and J. Li, “Highly sensitive electrogenerated chemiluminescence biosensor in profiling protein kinase activity and inhibition using gold nanoparticle as signal transduction probes,” *Analytical Chemistry*, vol. 82, no. 22, pp. 9566–9572, 2010.
- [28] D. Chen, X. Z. Zhou, and T. H. Lee, “Death-associated protein kinase 1 as a promising drug target in cancer and Alzheimer’s disease,” *Recent Patents on Anti-Cancer Drug Discovery*, vol. 14, no. 2, pp. 144–157, 2019.
- [29] S. M. Shah, F. Ullah, M. Ayaz, A. Wahab, and Z. K. Shinwari, “Phytochemical profiling and pharmacological evaluation of *Ifloga spicata* (FORSSK.) SCH. BIP. in leishmaniasis, lungs cancer and oxidative stress,” *Pakistan Journal of Botany*, vol. 51, pp. 2143–2152, 2019.
- [30] H. P. Borase, B. K. Salunke, R. B. Salunkhe et al., “Plant extract: a promising biomatrix for ecofriendly, controlled synthesis of silver nanoparticles,” *Applied Biochemistry and Biotechnology*, vol. 173, no. 1, pp. 1–29, 2014.
- [31] M. M. Khalil, E. H. Ismail, K. Z. El-Baghdady, and D. Mohamed, “Green synthesis of silver nanoparticles using olive leaf extract and its antibacterial activity,” *Arabian Journal of Chemistry*, vol. 7, no. 6, pp. 1131–1139, 2014.
- [32] K. Jemal, B. Sandeep, and S. Pola, “Synthesis, characterization, and evaluation of the antibacterial activity of *Allophylus serratus* leaf and leaf derived callus extracts mediated silver nanoparticles,” *Journal of Nanomaterials*, vol. 2017, 11 pages, 2017.
- [33] R. Gul, A. Badshah, A. A. Altaf, S. Tabassum, and M. Zia, “New ferrocenyl guanidines as potent antioxidants, protein kinase inhibitors and cytotoxic agents against human leukemia THP-1 cell line,” *Russian Journal of General Chemistry*, vol. 87, no. 11, pp. 2684–2689, 2017.



- [34] S. S. Shankar, A. Rai, A. Ahmad, and M. Sastry, "Rapid synthesis of Au, Ag, and bimetallic Au core–Ag shell nanoparticles using Neem (*Azadirachta indica*) leaf broth," *Journal of Colloid and Interface Science*, vol. 275, no. 2, pp. 496–502, 2004.
- [35] P. Banerjee, M. Satapathy, A. Mukhopahayay, and P. Das, "Leaf extract mediated green synthesis of silver nanoparticles from widely available Indian plants: synthesis, characterization, antimicrobial property and toxicity analysis," *Biore-sources and Bioprocessing*, vol. 1, no. 1, pp. 1–10, 2014.
- [36] M. Ghaffari-Moghaddam, R. Hadi-Dabanlou, M. Khajeh, M. Rakhshanipour, and K. Shameli, "Green synthesis of silver nanoparticles using plant extracts," *Korean Journal of Chemical Engineering*, vol. 31, no. 4, pp. 548–557, 2014.
- [37] A. Baranwal, A. K. Chiranjivi, A. Kumar, V. K. Dubey, and P. Chandra, "Design of commercially comparable nanotherapeutic agent against human disease-causing parasite, Leishmania," *Scientific Reports*, vol. 8, no. 1, pp. 1–10, 2018.
- [38] C. Krishnaraj, E. Jagan, S. Rajasekar, P. Selvakumar, P. Kalaichelvan, and N. Mohan, "Synthesis of silver nanoparticles using *Acalypha indica* leaf extracts and its antibacterial activity against water borne pathogens," *Colloids and Surfaces B: Biointerfaces*, vol. 76, no. 1, pp. 50–56, 2010.
- [39] B. Mehta, M. Chhajlani, and B. Shrivastava, "Green synthesis of silver nanoparticles and their characterization by XRD," *Journal of Physics: Conference Series*, vol. 836, article 012050, 2017.
- [40] D. Jain, H. K. Daima, S. Kachhwaha, and S. Kothari, "Synthesis of plant-mediated silver nanoparticles using papaya fruit extract and evaluation of their anti microbial activities," *Digest Journal of Nanomaterials and Biostructures*, vol. 4, pp. 557–563, 2009.
- [41] I. Khan, S. Tabassum, M. Ikram, and M. Zia, "Antioxidant, cytotoxicity, protein kinase inhibition and antibacterial activities of *Fragaria ananassa* leaves," *Pakistan Journal of Pharmaceutical Sciences*, vol. 31, 6 (Supplementary, pp. 2719–2723, 2018.
- [42] Y. M. Khan, *Phytochemical Investigation and Pharmacological Assessment of *Taverniera Nummularia* and *Ifloga Spicata**, University of Science and Technology, Bannu, 2019.
- [43] N. Narayanan, P. Thirugnanasambantham, S. Viswanathan, M. K. Reddy, V. Vijayasekaran, and E. Sukumar, "Antipyretic, antinociceptive and anti-inflammatory activity of *Premna herbacea* roots," *Fitoterapia*, vol. 71, no. 2, pp. 147–153, 2000.
- [44] S. Kumar, M. Singh, D. Halder, and A. Mitra, "Mechanistic study of antibacterial activity of biologically synthesized silver nanocolloids," *Colloids and Surfaces A: Physicochemical and Engineering Aspects*, vol. 449, pp. 82–86, 2014.
- [45] G. Yao, F. M. Sebisubi, L. Y. C. Voo, C. C. Ho, G. T. Tan, and L. C. Chang, "Citricin derivatives from the soil filamentous fungus *Penicillium* sp. H 9318," *Journal of the Brazilian Chemical Society*, vol. 22, no. 6, pp. 1125–1129, 2011.